General Disclaimer

One or more of the Following Statements may affect this Document

- This document has been reproduced from the best copy furnished by the organizational source. It is being released in the interest of making available as much information as possible.

- This document may contain data, which exceeds the sheet parameters. It was furnished in this condition by the organizational source and is the best copy available.

- This document may contain tone-on-tone or color graphs, charts and/or pictures, which have been reproduced in black and white.

- This document is paginated as submitted by the original source.

- Portions of this document are not fully legible due to the historical nature of some of the material. However, it is the best reproduction available from the original submission.

Produced by the NASA Center for Aerospace Information (CASI)

NASA TECHNICAL MEMORANDUM

NASA TM X-73923

NASA TM X-73923

(NASA-TM-X-73923) FRACTURE ANALYSIS OF SURFACE AND THROUGH-CRACKS IN CYLINDRICAL PRESSURE VESSELS (NASA) 43 p HC $4.00 CSCL 13M

N76-26580

Unclas

G3/39 44516

FRACTURE ANALYSIS OF SURFACE- AND THROUGH-CRACKS IN CYLINDRICAL PRESSURE VESSELS

BY
J. C. Newman, Jr.
Langley Research Center
Hampton, VA 23665

TECHNICAL PAPER to be presented at the ASME International Joint Pressure Vessels, Piping, and Petroleum Engineering Conference, September 19 - 24, 1976, Mexico City, Mexico

This informal documentation medium is used to provide accelerated or special release of technical information to selected users. The contents may not meet NASA formal editing and publication standards, may be revised, or may be incorporated in another publication.

NATIONAL AERONAUTICS AND SPACE ADMINISTRATION
LANGLEY RESEARCH CENTER, HAMPTON, VIRGINIA 23665

JUL 1976
RECEIVED
NASA STI FACILITY
INPUT BRANCH

1. Report No.	2. Government Accession No.	3. Recipient's Catalog No.
NASA TM X-73923		

4. Title and Subtitle	5. Report Date
FRACTURE ANALYSIS OF SURFACE- AND THROUGH-CRACKS IN CYLINDRICAL PRESSURE VESSELS	6. Performing Organization Code: 2532
7. Author(s): James C. Newman, Jr.	8. Performing Organization Report No.
9. Performing Organization Name and Address: NASA-Langley Research Center, Hampton, VA 23665	10. Work Unit No.: 505-02-31-01
	11. Contract or Grant No.
12. Sponsoring Agency Name and Address: National Aeronautics and Space Administration, Washington, DC 20546	13. Type of Report and Period Covered: Technical Memorandum
	14. Sponsoring Agency Code

15. Supplementary Notes

Paper to be presented at the ASME International Joint Pressure Vessels, Piping, and Petroleum Engineering Conference, Sept. 19-24, 1976, Mexico City, Mexico

16. Abstract

A previously developed fracture criterion was applied to surface- and through-cracked cylindrical pressure vessels to see how well the criterion can correlate fracture data. Fracture data from the literature on surface cracks in aluminum alloy, steel, and epoxy vessels and on through cracks in aluminum alloy, titanium alloy, steel, and brass vessels were analyzed using the fracture criterion. The criterion correlated the failure stresses to within ±10 percent for either surface or through cracks over a wide range of crack size and vessel diameter. The fracture criterion was also found to correlate failure stresses from flat plates (center-crack or double-edge-crack tension specimens) and cylindrical pressure vessels containing through cracks within ±10 percent.

17. Key Words (Suggested by Author(s)) (STAR category underlined)	18. Distribution Statement
Fracture Stress-Intensity Factor Structural Mechanics Materials (Metallic)	Unclassified - Unlimited

19. Security Classif. (of this report)	20. Security Classif. (of this page)	21. No. of Pages	22. Price*
Unclassified	Unclassified	39	$3.75

*Available from: The National Technical Information Service, Springfield, Virginia 22151; STIF/NASA Scientific and Technical Information Facility, P.O. Box 33, College Park, MD 20740

FRACTURE ANALYSIS OF SURFACE-AND THROUGH-CRACKS IN CYLINDRICAL PRESSURE VESSELS

By

J. C. Newman, Jr.

NASA Langley Research Center

Hampton, Virginia 23665, U.S.A.

ABSTRACT

A previously develcped fracture criterion was applied to surface- and through-cracked cylindrical pressure vessels to see how well the criterion can correlate fracture data. Fracture data from the literature on surface cracks in aluminum alloy, steel, and epoxy vessels and on through cracks in aluminum alloy, titanium alloy, steel, and brass vessels were analyzed using the fracture criterion. The criterion correlated the failure stresses to within ±10 percent for either surface or through cracks over a wide range of crack size and vessel diameter. The fracture criterion was also found to correlate failure stresses from flat plates (center-crack or double-edge-crack tension specimens) and cylindrical pressure vessels containing through cracks within ± 10 percent.

INTRODUCTION

Failures of many pressure vessels have been traced to surface cracks or to through cracks. These cracks initiate at structural discontinuities such as holes, material defects, or other abrupt changes in configuration and may propagate to failure under operating stress levels. In designing to prevent such failures, the designer must be able to predict the effects of crack size on structural strength. Linear-Elastic Fracture Mechanics (LEFM), which utilizes the concept of the elastic stress-intensity factor, has been used to correlate fracture data and predict failure for cracked plates and structural components when the crack-tip plastic deformations are constrained to small regions (plane-strain fracture [1]). However, when plastic deformations near the crack tip are large (plastic zone greater than plate thickness) the elastic stress-intensity factor at failure (K_{Ie}) varies with crack size and structural dimensions [2-4]. To account for the variation in K_{Ie} with structural dimensions, the elastic-plastic stress-strain behavior at the crack tip must be considered.

An equation which accounts for the effects of plastic deformation on fracture was derived in references [4] and [5]. This equation relates K_{Ie} to the elastic nominal failure stress and two material fracture parameters and is designated the Two-Parameter Fracture Criterion (TPFC). The TPFC has correlated fracture data for surface- and through-cracks, for different specimen types, and for a wide range of materials [4-7].

The purpose of the present paper is to apply the TPFC to surface- and through-cracked cylindrical shells subjected to internal pressure (Fig. 1)

to see how well the TPFC can correlate such fracture data. Fracture data for pressurized cylinders made of various materials (aluminum alloy, titanium alloy, steel, brass and epoxy) were taken from the literature (see Table I). Some of the literature sources reported fracture data on flat plates (Fig. 2) in addition to the data for cylinders. To determine if the failure stresses in the cylinders may be predicted using fracture data for the flat plates, experimental and predicted failure stresses in the flat plates were compared. The predicted failure stresses were computed using the two material fracture parameters determined from the cylinder data. In order to apply the TPFC to fracture data, the elastic stress-intensity factors for these crack configurations must be known.

The elastic stress-intensity factors for through cracks in pressurized cylinders have been obtained theoretically by Folias [18] and Erdogan and Kibler [19] for crack lengths less than about five times the square root of the product of vessel radius and thickness. In the present paper an empirical equation giving elastic stress-intensity factors for through cracks has been obtained using the numerical results from [19] and some experimental fracture tests on brass vessels [16]. The resulting equation applies over a range of crack lengths about twice as large as those considered in [18] and [19].

The elastic stress-intensity factors for surface cracks in pressurized cylinders have not been obtained theoretically, but some experimental stress-intensity factors have been determined from surface cracks in brittle epoxy vessels [17]. In the present paper an empirical equation giving elastic stress-intensity factors for surface cracks has been developed using the results from [4] and [19]. The results from this equation are compared with the experimental stress-intensity factors from [17].

SYMBOLS

a	initial depth of surface crack, m
c	initial half-length of surface or through crack, m
f	shell-curvature correction factor for a through crack
f_s	shell-curvature correction factor for a surface crack
F	complete boundary correction on the stress-intensity factor
H	height of uniformly-stressed specimens, m
K_F	fracture-toughness parameter, $N/m^{3/2}$
K_I	elastic stress-intensity factor, $N/m^{3/2}$
K_{Ie}	elastic stress-intensity factor at failure, $N/m^{3/2}$
M_e	combined front-face and back-face correction on the stress-intensity factor for the surface crack
M_1	front-face correction on the stress-intensity factor for the surface crack
m	fracture-toughness parameter
p	internal pressure, N/m^2
Q	elastic surface-crack shape factor
R	radius of cylindrical pressure vessel, m
S	gross stress, N/m^2
S_n	nominal stress at failure in cracked plate or cylinder, N/m^2
S_u	nominal stress required to fail the uncracked plate or vessel ($S_u = \sigma_u$ for center-crack and double-edge-crack tension specimens and $S_u = 1.15\ \sigma_u$ for pressurized cylinders)
T	temperature, K

t	shell thickness, m
W	specimen width, m
λ	through-crack shell parameter, $\frac{c}{\sqrt{Rt}}$
λ_s	surface-crack shell parameter, $\frac{c}{\sqrt{Rt}} \left(\frac{a}{t}\right)$
ν	Poisson's ratio
σ_u	uniaxial tensile strength, N/m^2
σ_{ys}	uniaxial yield stress, N/m^2
ϕ	ratio of K_{Ie} to K_F

TWO-PARAMETER FRACTURE CRITERION

The Two-Parameter Fracture Criterion (TPFC) was developed and successfully applied to plane fracture specimens containing either surface- or through-cracks in metallic materials [4-7]. The TPFC accounts for the effects of plastic deformation on fracture properties. The equation is

$$K_F = \frac{K_{Ie}}{1 - m\left(\frac{S_n}{S_u}\right)} \quad \text{for} \quad S_n \leq \sigma_{ys} \tag{1}$$

where K_{Ie} is the elastic stress-intensity factor at failure, S_n is the nominal (net-section) failure stress, S_u is the nominal stress required to fail the uncracked vessel, and K_F and m are the two material fracture parameters. The fracture parameters K_F and m are assumed to be constant for a given combination of material, thickness, temperature, and rate of loading. To obtain fracture parameters that are representative for a given material and test temperature: (1) the nominal failure stress must be less than σ_{ys}, (2) the fracture data must all be from the same specimen thickness, and (3) the test data must encompass a wide range of crack lengths or specimen sizes. Reference 4 shows how the fracture parameters are determined by a least-squares procedure for a given set of fracture data. To define the complete fracture behavior for a material, K_F and m must be determined as functions of thickness, temperature and load rate.

If m equals zero in equation (1), K_F equals the elastic stress-intensity factor at failure and the equation applies to low-toughness (low K_F) materials (plane-strain fracture). However, if m equals unity, the equation applies to extremely ductile or high-toughness (high K_F)

materials. Thus, the fracture parameters, K_F and m, jointly describe the crack sensitivity of the material.

The denominator in equation (1) reflects the influence of the nominal failure stress on fracture toughness. The variation of the denominator with nominal stress for a typical material is shown in Figure 3. When the nominal stress is less than the uniaxial yield stress, σ_{ys}, the function ϕ (ratio of K_{Ie} to K_F) is a linear function of nominal stress (solid line). However, when the nominal failure stress is greater than the yield stress, the function ϕ becomes nonlinear and is dependent upon the stress-strain curve of the material and the state of stress in the crack-tip region, as discussed in [4, 6]. For thin materials, where the state of stress in the crack-tip region is biaxial, the expected behavior is estimated by the dash-dot curve. An equation approximating the dash-dot curve is given in [6] by

$$\phi = \frac{K_{Ie}}{K_F} = \frac{\sigma_{ys}}{S_n}\left(1 - m\frac{S_n}{S_u}\right) \quad \text{for} \quad \sigma_{ys} < S_n < S_u \tag{2}$$

and is shown in Figure 3 as the dashed curve. For thick materials, where the state of stress in the crack-tip region is triaxial, the fracture behavior for $S_n > \sigma_{ys}$ is expected to lie closer to the solid line. The solid vertical line truncates the nominal stress at S_u. In this paper, equation (2) was used whenever S_n was greater than σ_{ys}.

In order to apply equation (1) to surface- and through-cracks in pressurized cylinders, the nominal stress required to fail the uncracked vessel, S_u, and the elastic stress-intensity factor, K_{Ie}, for these configurations must be determined. For pressurized cylinders, S_u was 1.15 times the ultimate tensile strength (σ_u). It was determined by calculating the

nominal (hoop) stress required to satisfy the Mises yield criterion (where the yield stress was replaced by σ_u) assuming a 2:1 biaxial stress ratio. The elastic stress-intensity factor equations for these configurations are presented in the next section.

ELASTIC STRESS-INTENSITY FACTORS

The form of the elastic stress distribution near a crack tip that contains the stress-intensity factor, K_I, and the square-root singularity is well known [2]. (The determination of K_I is the basis for Linear-Elastic Fracture Mechanics.) The stress-intensity factor is a function of load, structural configuration, and the size, shape, and location of the crack. In general, the elastic stress-intensity factor can be expressed as

$$K_{Ie} = S_n \sqrt{\pi c}\, F \tag{3}$$

for any Mode I crack configuration where S_n is the nominal stress, c is the initial crack length (defined in Figure 1), and F is the boundary-correction factor. The boundary-correction factor accounts for the influence of various boundaries and crack shape on stress intensity. The following sections give the nominal stress equation and the boundary-correction factor equations for the surface- and through-cracked cylindrical pressure vessel.

Through Crack in a Pressurized Cylinder

For the through crack (axial) in a cylindrical shell subjected to internal pressure, Figure 1(a), the elastic stress-intensity factor at failure is given by equation (3) where the nominal stress is

$$S_n = \frac{pR}{t} \tag{4}$$

and

$$F = f = [1 + 0.52\,\lambda + 1.29\,\lambda^2 - 0.074\,\lambda^3]^{1/2} \tag{5}$$

for $0 \leq \lambda \leq 10$ where $\lambda = c/\sqrt{Rt}$. Equation (5) accounts for the effects of shell curvature [18, 19] on stress intensity. Poisson's ratio was assumed to be 1/3. The details on the development of equation (5) are given in the Appendix.

Surface Crack in a Pressurized Cylinder

For the internal or external surface crack (axial) in a cylindrical shell subjected to internal pressure, Figure 1(b), the elastic stress-intensity factor at failure is also given by equation (3), where the nominal stress is given by equation (4) and

$$F = \sqrt{\frac{a}{cQ}}\, M_e\, f_s \tag{6}$$

The square-root term converts the through-crack expression to that for a surface-crack, M_e is the combined front-face and back-face correction factor, and f_s is the shell-curvature correction factor for a surface crack. The elastic shape factor, Q, was given in [20] as the square of the elliptic integral of the second kind. An expression was chosen in [4] as a simple approximation for Q and is given by

$$\left.\begin{aligned} Q &= 1 + 1.47\left(\frac{a}{c}\right)^{1.64} \quad \text{for } \frac{a}{c} \leq 1.0 \\ Q &= 1 + 1.47\left(\frac{c}{a}\right)^{1.64} \quad \text{for } \frac{a}{c} > 1.0 \end{aligned}\right\} \tag{7}$$

The expression for M_e was developed in [4] and is given by

$$M_e = [M_1 + (\sqrt{Q}\,\frac{c}{a} - M_1)(\frac{a}{t})^q] \tag{8}$$

where q was determined empirically in [4] as

$$q = 2 + 8\,(\frac{a}{c})^3 \tag{9}$$

The term M_1 is the front-face correction, the $\frac{a}{t}$ term is the backface correction. The expression for M_1 is given by

$$\left.\begin{aligned} M_1 &= 1.13 - 0.1\,(\frac{a}{c}) \quad \text{for} \quad 0.02 \leq \frac{a}{c} \leq 1.0 \\ M_1 &= \sqrt{\frac{c}{a}}\,(1 + 0.03\,\frac{c}{a}) \quad \text{for} \quad \frac{a}{c} > 1.0 \end{aligned}\right\} \tag{10}$$

The shell-curvature correction factor for a surface crack, f_s, is given by

$$f_s = [1 + 0.52\,\lambda_s + 1.29\,\lambda_s^2 - 0.074\,\lambda_s^3]^{1/2} \tag{11}$$

for $0 \leq \lambda_s \leq 10$ where $\lambda_s = \frac{c}{\sqrt{Rt}}\frac{a}{t}$. Again, Poisson's ratio was assumed to be 1/3. The form of λ_s was obtained by assuming that the surface crack could be replaced by an "equivalent" through crack of equal area. As $\frac{a}{t}$ approaches unity, λ_s approaches λ and equation (6) reduces to equation (5). In the Appendix, equation (6) is compared with some experimentally determined correction factors for a brittle epoxy.

Through Crack in Axially Loaded Flat Plates

Center-crack tension.- For the center-crack tension specimen (Fig. 2(a)), the elastic stress-intensity factor is given by equation (3) where

$$S_n = \frac{S}{1 - \frac{2c}{W}} \tag{12}$$

and

$$F = \left(1 - \frac{2c}{W}\right) \sqrt{\sec \frac{\pi c}{W}} \tag{13}$$

for $0 \leq \frac{2c}{W} < 1.0$ and $H/W \geq 2$. The secant term is the finite-width correction on stress-intensity factor and was obtained from [1].

Double-edge-crack tension.- For the double-edge-crack tension specimen (Fig. 2(b)), the elastic stress-intensity is given by equation (3), where S_n is given by equation (12), and F was obtained by a boundary-collocation analysis of a configuration with $H/W = 0.625$. (Fracture data analyzed from [15] used this particular configuration.) The stress S was assumed to be uniformly applied. An equation fit to the collocation results gave

$$F = 1.13 \left(1 - \frac{2c}{W}\right) \sqrt{\sec \frac{\pi c}{W}} \tag{14}$$

for $0 \leq \frac{2c}{W} \leq 0.4$ and $H/W = 0.625$. (Stress-intensity factors for H/W ratios of 1, 3 and infinity are given in [2].)

ANALYSIS OF FRACTURE DATA

Fracture data on pressurized cylinders made of various materials and containing either surface- or through-cracks were taken from the literature and were analyzed using the TPFC (eqns. (1) and (2)). The fracture parameters K_F and m, for a given material, thickness, and test temperature were determined from the fracture data using a best-fit procedure described in [4]. These values of K_F and m were then used to calculate failure stresses for the same fracture tests to see how well the TPFC correlated the failure stresses. Where fracture data on flat plates (center-crack tension or edge-crack tension) were available, experimental and predicted failure stresses for the flat plates were compared. The failure stresses were computed using the two material fracture parameters determined from the cylinder data. The failure stresses were calculated by substituting equation (3) into equations (1) and (2), and were given by

$$S_n = \frac{K_F}{\sqrt{\pi c}\ F + \frac{m\ K_F}{S_u}} \quad \text{for} \quad S_n \leq \sigma_{ys} \tag{15}$$

and

$$S_n = \sqrt{(m\gamma)^2 + 2\gamma S_u} - m\gamma \quad \text{for} \quad \sigma_{ys} < S_n < S_u \tag{16}$$

where

$$\gamma = \frac{K_F\ \sigma_{ys}}{2S_u\ \sqrt{\pi c}\ F} \tag{17}$$

Table I summarizes the materials, thicknesses, test temperatures and crack configurations that were analyzed. Figures 4-15 show the correlation obtained for each set of fracture data. Table I also indicates which fracture data were obtained using sharp saw-cut slits instead of fatigue cracks.

Through Cracks

Pressurized cylinders.- Figures 4-7 show fracture data on pressurized cylinders containing through cracks. The figures show the nominal failure stress normalized to S_u $(1.15\ \sigma_u)$ plotted against half length of crack, c. The symbols show the fracture data and the curves are best fits of the TPFC using the values of K_F and m determined from these data. A knee occurs in all curves when the nominal stress is equal to the yield stress of the material (transition from equation (15) to equation (16)), but some are hardly perceptible. The calculated failure stresses were generally within $\pm$ 10 percent of the experimental failure stresses.

Pressurized cylinders and flat plates.- Figures 8-13 show fracture data on pressurized cylinders and flat plates made of the same material and thickness and tested at the same temperature. Both the cylinders and flat plates contained through cracks. The figures show nominal failure stress normalized to S_u plotted against half length of crack, c. For the flat plates $S_u = \sigma_u$ and for the cylinders $S_u = 1.15\ \sigma_u$. The fracture parameters, K_F and m, were determined from an analysis of the fracture data on the pressurized cylinders. The fracture data on the flat plates were insufficient to obtain the two parameters because only one specimen size and crack length was tested. The solid curve or curves show the calculations from the TPFC

for various vessel radii. The agreement was considered good. The dashed curve on each figure shows the predicted results for flat plates ($R = \infty$) using the values of K_F and m determined from the cylinders. The circular symbols show the experimental results for the flat plates. The predicted results were within $\pm$ 10 percent of the experimental failure stresses.

Surface Cracks

Pierce [11] conducted cryogenic fracture tests on surface cracks in 2014-T6 material. Figure 14 shows the nominal failure stress normalized to S_u ($1.15\ \sigma_u$) plotted against cF^2, where c is the half length of crack and F is the boundary-correction factor (eqn. (6)). The TPFC indicates that this type of plot ($\frac{S_n}{S_u}$ against cF^2) gives a single curve for various $\frac{a}{c}$ and $\frac{a}{t}$ ratios. The open and solid circular symbols denote experimental data on externally or internally located surface cracks, respectively. The surface crack data included variations in crack shape ($0.07 \leq \frac{a}{c} \leq 0.9$) and crack size ($0.36 \leq \frac{a}{t} \leq 0.98$). The curve shows the calculations from the TPFC using the values of K_F and m determined from these data. The calculated failure stresses were within $\pm$ 10 percent of the experimental failure stresses.

Kiefner, Maxey, Eiber, and Duffy [14] conducted surface-crack fracture tests at room temperature on steel pressure vessels. Figure 15 shows the nominal failure stresses normalized to S_u plotted against cF^2. The surface-crack data included variations in crack shape ($0.02 \leq \frac{a}{c} \leq 0.14$) and crack size ($0.38 \leq \frac{a}{t} \leq 0.82$). The symbols denote the fracture data and the curve shows the calculations from the TPFC. The agreement was considered good.

CONCLUDING REMARKS

A Two-Parameter Fracture Criterion (TPFC) that relates the elastic stress-intensity at failure, the elastic nominal failure stress, and two material parameters was used to analyze fracture data on surface-cracked and through-cracked cylindrical pressure vessels. Fracture data from the literature on steel, titanium alloy, aluminum alloy, brass, or epoxy vessels tested at either room or cryogenic temperature were analyzed. The TPFC correlated the data well (generally within $\pm$ 10 percent of the experimental failure stresses) for a broad range of materials, including some that were extremely ductile. The fracture criterion was also found to correlate fracture data from flat plates and cylindrical pressure vessels within $\pm$ 10 percent for the same material, thickness, and test temperature.

APPENDIX

DEVELOPMENT AND VERIFICATION OF BOUNDARY CORRECTIONS ON STRESS-INTENSITY FACTORS

Through Cracks

Folias [18] and Erdogan and Kibler [19] have obtained the elastic stress-intensity factors for a longitudinal (axial) through crack in a pressurized cylinder (Fig. 1(a)) for $\lambda \leq 4.5$. Figure 16 shows the shell-curvature correction (or boundary-correction factor) on stress intensity as a function of λ. The symbols are numerical values obtained from [19] for $\nu = 1/3$. The shell-curvature correction factor, F, was determined by

$$F = F_T + \frac{1}{2} |F_B| \tag{16}$$

where F_T is the contribution due to the membrane solution (or normal forces) and F_B is the contribution due to bending. Reference 21 has shown that including one half of the bending contribution was necessary to correlate crack-growth rates from pressurized cylinders and flat plates. The bending term contributed only about 10 percent to the total correction factor.

The solid curve in Figure 16 is an equation chosen herein (eqn. (5)) to fit the numerical values. The solid curve was within $\pm$ 5 percent of the numerical values. Reference 21 has shown that the effects of Poisson's ratio (ν = 0 to 0.5) on the curvature correction was less than 5 percent from the values given in Figure 16. Therefore, equation (5) was assumed to apply for any material.

For $\lambda > 4.5$, an experimental technique was used herein to verify the applicability of equation (5) for calculating the shell-curvature correction factors. Figure 17 shows the curvature correction factor plotted against λ. The symbols show the experimentally derived correction factors from through crack fracture data on brass cylinders [16] using the TPFC. The correction factors are given by

$$f = F = \frac{K_F \left(1 - m \frac{S_n}{S_u}\right)}{S_n \sqrt{\pi c}} \tag{17}$$

The fracture parameters, K_F and m, were determined from an analysis of the fracture data with $\lambda \leq 4$. The crack length, c, and the corresponding failure stresses, S_n, were obtained from [16]. The solid curve shows the correction factors calculated from equation (5). The solid curve is in good agreement with the experimental data. Therefore, equation (5) was assumed to apply for any material with $\lambda \leq 10$.

Surface Crack

Derby [17] has experimentally determined stress-intensity correction factors for surface cracks in pressurized cylinders made of a brittle epoxy. The critical elastic stress-intensity factor for this material, $K_{Ie} = 1.02$ $MN/m^{3/2}$, was obtained from four-point notch bend fracture tests [17]. This material was brittle (m = 0). The experimental correction factors for the surface cracks were obtained from equation (3) as

$$F = \frac{K_{Ie}}{S_n \sqrt{\pi c}} = \frac{1.02}{S_n \sqrt{\pi c}} \tag{18}$$

where S_n and c were obtained from the fracture tests on the epoxy vessels. Table II shows a comparison between the experimentally determined correction factors and those calculated from equation (6). The theoretical correction factors were within $\pm$ 10 percent of the experimental values.

REFERENCES

1. "Plane Strain Crack Toughness Testing of High Strength Metallic Materials", ASTM STP 410, 1966.

2. "Fracture Toughness", ASTM STP 381, 1964.

3. Kuhn, P.: Residual Tensile Strength in the Presence of Through Cracks or Surface Cracks, NASA TN D-5432, 1970.

4. Newman, J. C., Jr.: Fracture Analysis of Surface- and Through-Cracked Sheets and Plates, Engineering Fracture Mechanics Journal, vol. 5, 1973.

5. Newman, J. C., Jr.: Plane Stress Fracture of Compact and Notch-Bend Specimens, NASA TM X-71926, 1973.

6. Newman, J. C., Jr.: Fracture Analysis of Various Cracked Configurations in Sheet and Plate Materials, NASA TM X-72709, 1975.

7. Newman, J. C., Jr.: Predicting Failure of Specimens With Either Surface Cracks or Corner Cracks at Holes, NASA TN D-8244, 1976.

8. Peters, R. W.; and Kuhn, P.: Bursting Strength of Unstiffened Pressure Cylinders With Slits, NACA TN 3993, April 1957.

9. Anderson, R. B.; and Sullivan, T. L.: Fracture Mechanics of Through-Cracked Cylindrical Pressure Vessels, NASA TND-3252, Feb. 1966.

10. Sullivan, T. L.; and Pierce, W. S.: Effect of Radius on Bulging and Fracture of Through-Cracked Cylindrical Pressure Vessels at Cryogenic Temperatures, NASA TND-4951, Dec. 1968.

11. Pierce, W. S.: Effects of Surface and Through Cracks on Failure of Pressurized Thin-Walled Cylinders on 2014-T6 Aluminum, NASA TN D-6099, Nov. 1970.

12. Sullivan, T. L.: Texture Strengthening and Fracture Toughness of Titanium Alloy Sheet at Room and Cryogenic Temperatures, NASA TND-4444, May 1968.

13. Calfo, F. D.: Effects of Residual Stress on Fracture Strength of AISI 301 Stainless-Steel and Ti-5Al-2.5 Sn ELI Titanium Cracked Thin-Wall Cylinders, NASA TND-4777, Sept. 1968.

14 Kiefner, J. F.; Maxey, W. A.; Eiber, R. J.; and Duffy, A. R.: Failure Stress Levels of Flaws in Pressurized Cylinders, Progress in Flaw Growth and Fracture Toughness Testing, ASTM STP 536, American Society for Testing and Materials, 1973.

15. Kihara, H.; Ikeda, K.; and Iwanga, H.: Brittle Fracture Initiation of Line Pipe, Document X-371-66, Presented at Int. Inst. Welding, Delft, 1966.

16. Sechler, E. E.; and Williams, M. L.: The Critical Crack Length Pressurized Monocoque Cylinders, Graduate Aero. Lab. Cal. Inst. Tech. Report, Sept. 1959. (See also M. L. Williams in Proceedings of Crack Propagation Symposium, Cranfield, 1961.)

17. Derby, R. W.: Experimentally Determined Shape Factors for Deep Part-Through Cracks in a Thick-Walled Pressure Vessel, Progress in Flaw Growth and Fracture Toughness Testing, ASTM STP 536, American Society for Testing and Materials, 1973.

18. Folias, E. S.: An Axial Crack in a Pressurized Cylindrical Shell, International Journal of Fracture Mechanics, vol. 1, no. 2, June 1965.

19. Erdogan, F.; and Kibler, J. J.: Cylindrical and Spherical Shells with Cracks, International Journal of Fracture Mechanics, vol. 5, no. 3, Sept. 1969.

20. Irwin, G. R.: The Crack Extension Force for a Part-Through Crack in a Plate, Trans. ASME, J. Appl. Mech., 84, 651-654, 1962.

21. Erdogan, F.; and Ratawani, M.: Fracture of Cylindrical and Spherical Shells Containing a Crack, NASA-TR-71-3, July 1971.

TABLE I.- MATERIALS, THICKNESSES, TEST TEMPERATURES AND CRACK CONFIGURATIONS.

Material		Thickness mm	Temp. K	Pressurized cylinders		Flat plates	Ref.
				Surface crack	Through crack	Through crack	
AL	7075-T6	0.4-0.6	RT		X(a)		8
	2024-13	0.3-0.4	RT		X(a)		8
	2014-T6	1.5	RT		X(a)		9
	2014-T6	1.5	20		X	X	10
	2014-T6	1.5	77		X	X	10
	2014-T6	1.5	77	X			11
TI	5Al-2.5Sn	0.5	20		X	X	10
	5Al-2.5Sn	0.5	77		X	X	12
STEEL	301	0.6	RT		X		13
	X-52	9.5	RT		X(a)		14
	X-52	9.5	RT	X(a)			14
	Hot-rolled(b)	6.4	77		X	X	15
Brass		0.025	RT		X(a)		16
Brittle Epoxy		15	RT	X			17

(a) Sharp saw-cut slits instead of fatigue cracks

(b) 0.25C, 0.02Si, 0.85Mn

PRECEDING PAGE BLANK NOT FILMED

TABLE II. - COMPARISON OF THEORETICAL AND EXPERIMENTALLY DETERMINED BOUNDARY-CORRECTION FACTORS FOR SURFACE CRACKS IN PRESSURIZED CYLINDERS MADE OF A BRITTLE EPOXY [17] (a)

a mm	c mm	EXPERIMENT F	THEORY F	THEORY / EXPERIMENT
13.2	14.6	0.959	0.932	0.97
12.2	14.2	0.878	0.863	0.98
11.1	14.5	0.846	0.855	1.01
10.9	14.5	0.846	0.823	0.97
10.5	15.9	0.808	0.841	1.04
11.5	14.4	0.831	0.839	1.01
10.7	14.5	0.785	0.819	1.04
6.9	9.5	0.682	0.696	1.02
6.9	8.3	0.708	0.689	0.97
7.3	8.3	0.672	0.689	1.03
5.4	8.5	0.621	0.677	1.09

(a) R = 68.3 mm and t = 15 mm

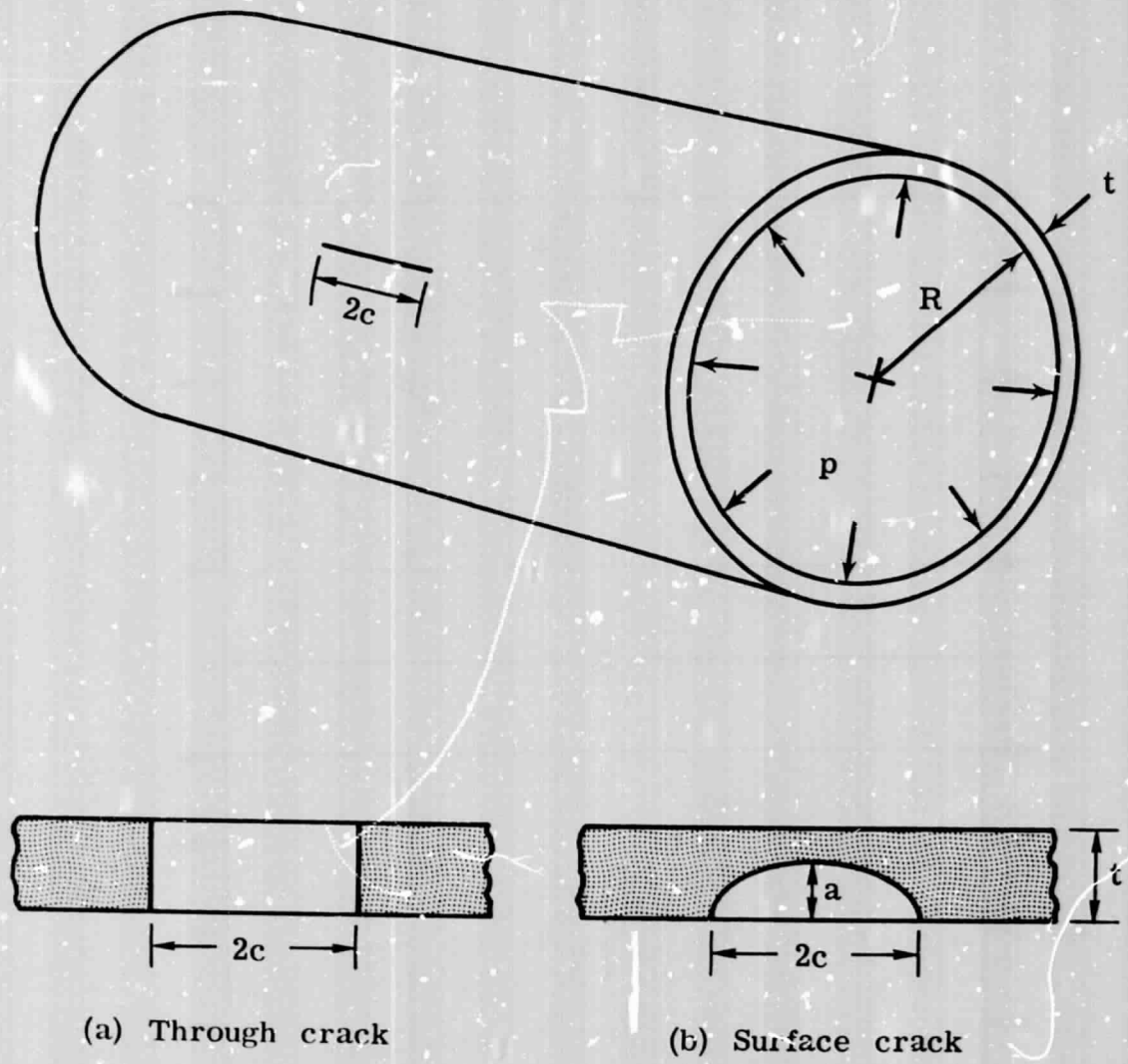

Figure 1.-- Surface crack or a through crack in a pressurized cylinder.

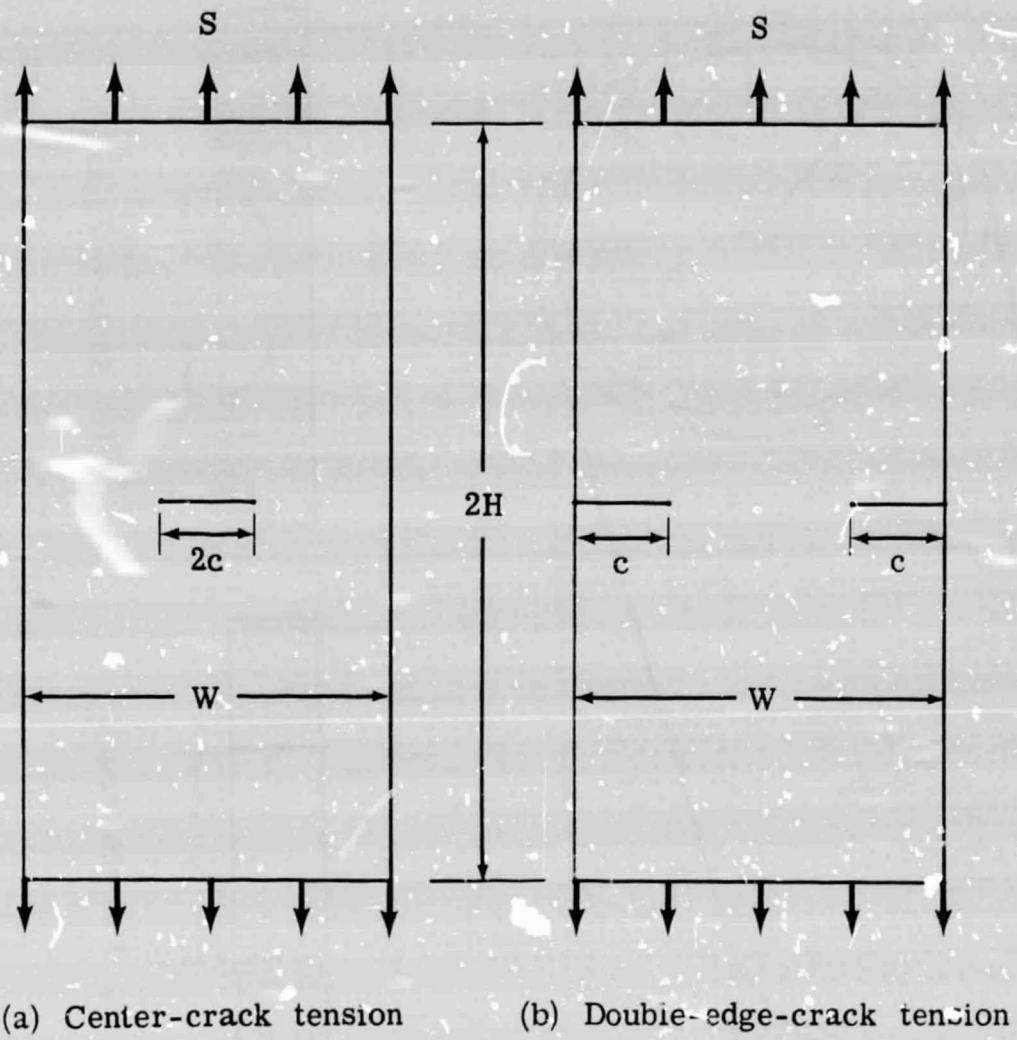

Figure 2.- Through-crack configurations in flat plates.

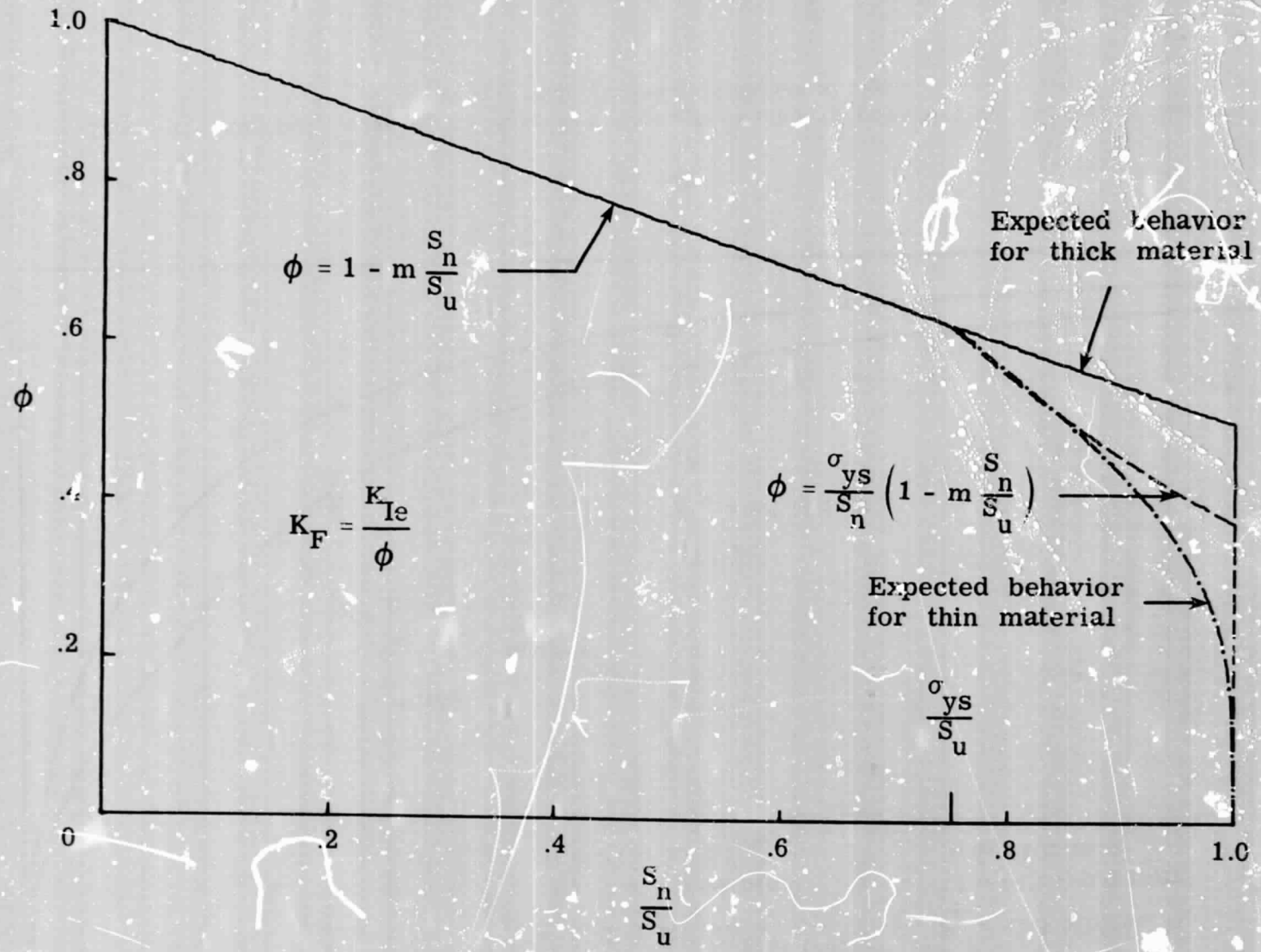

Figure 3.- Typical relationship between ϕ and S_n/S_u.

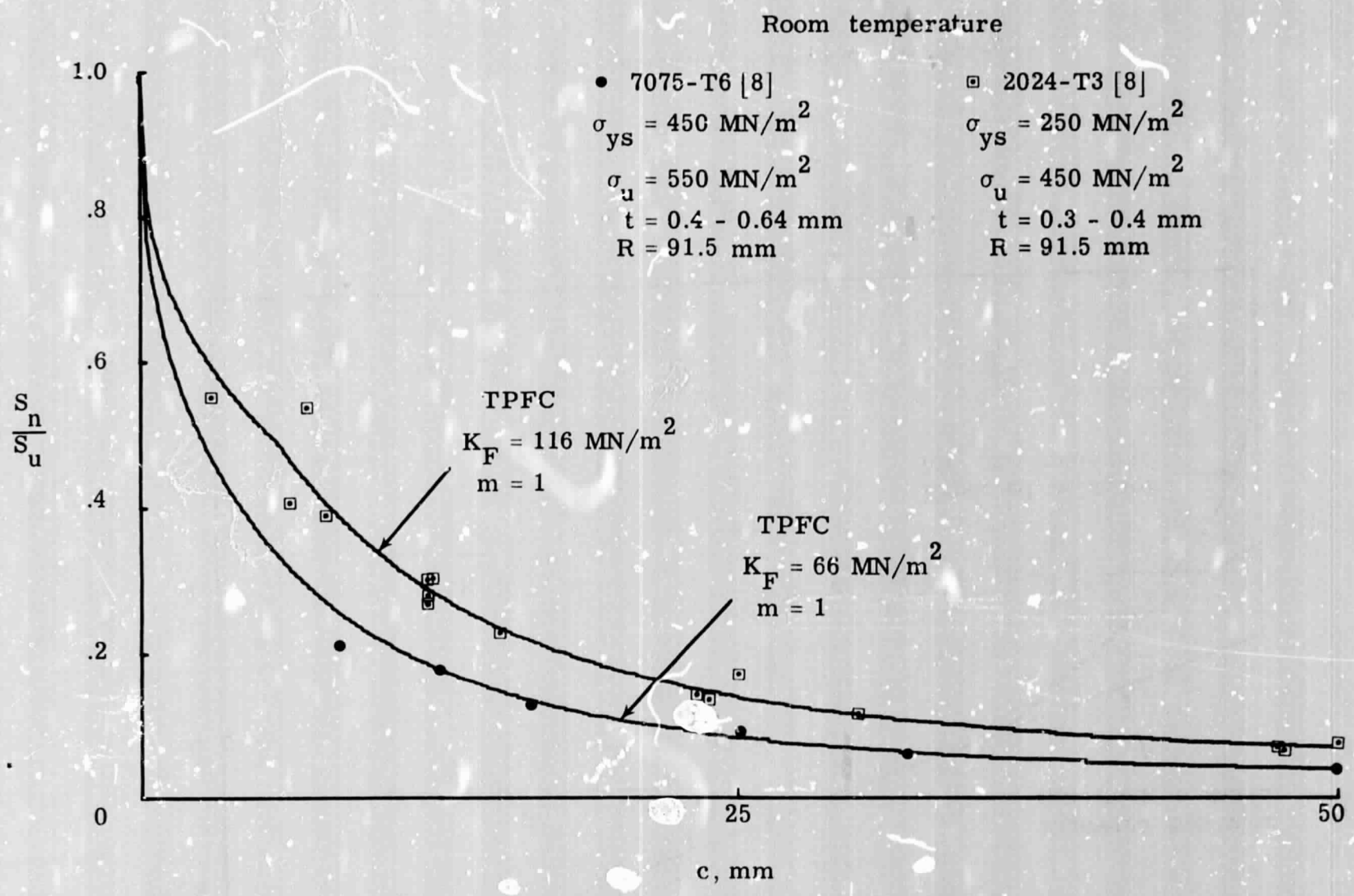

Figure 4.- Nominal failure stresses for through cracks in pressurized cylinders made of 7075-T6 and 2024-T3 aluminum alloy.

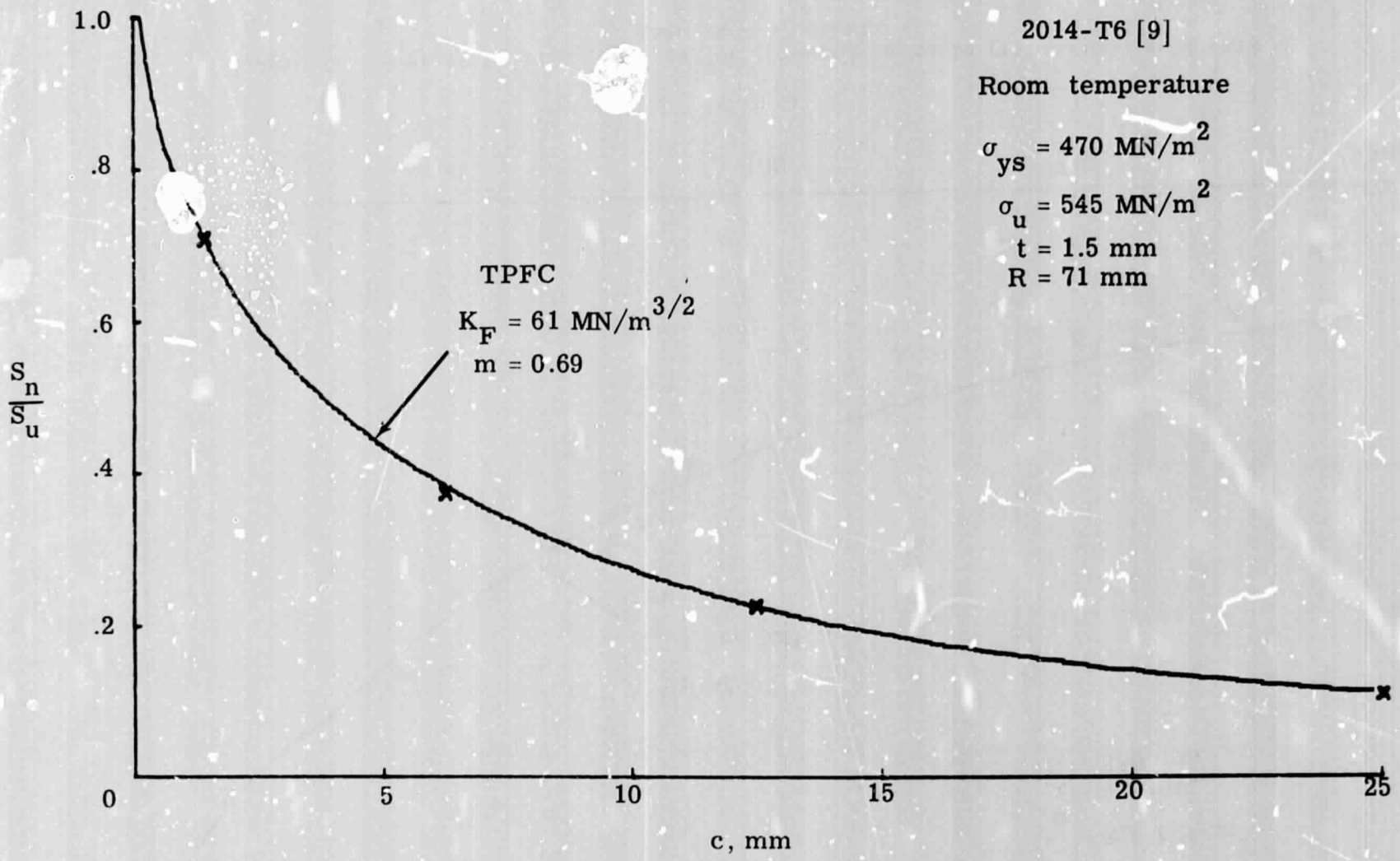

Figure 5.- Nominal failure stresses for through cracks in pressurized cylinders made of 2014-T6 aluminum alloy.

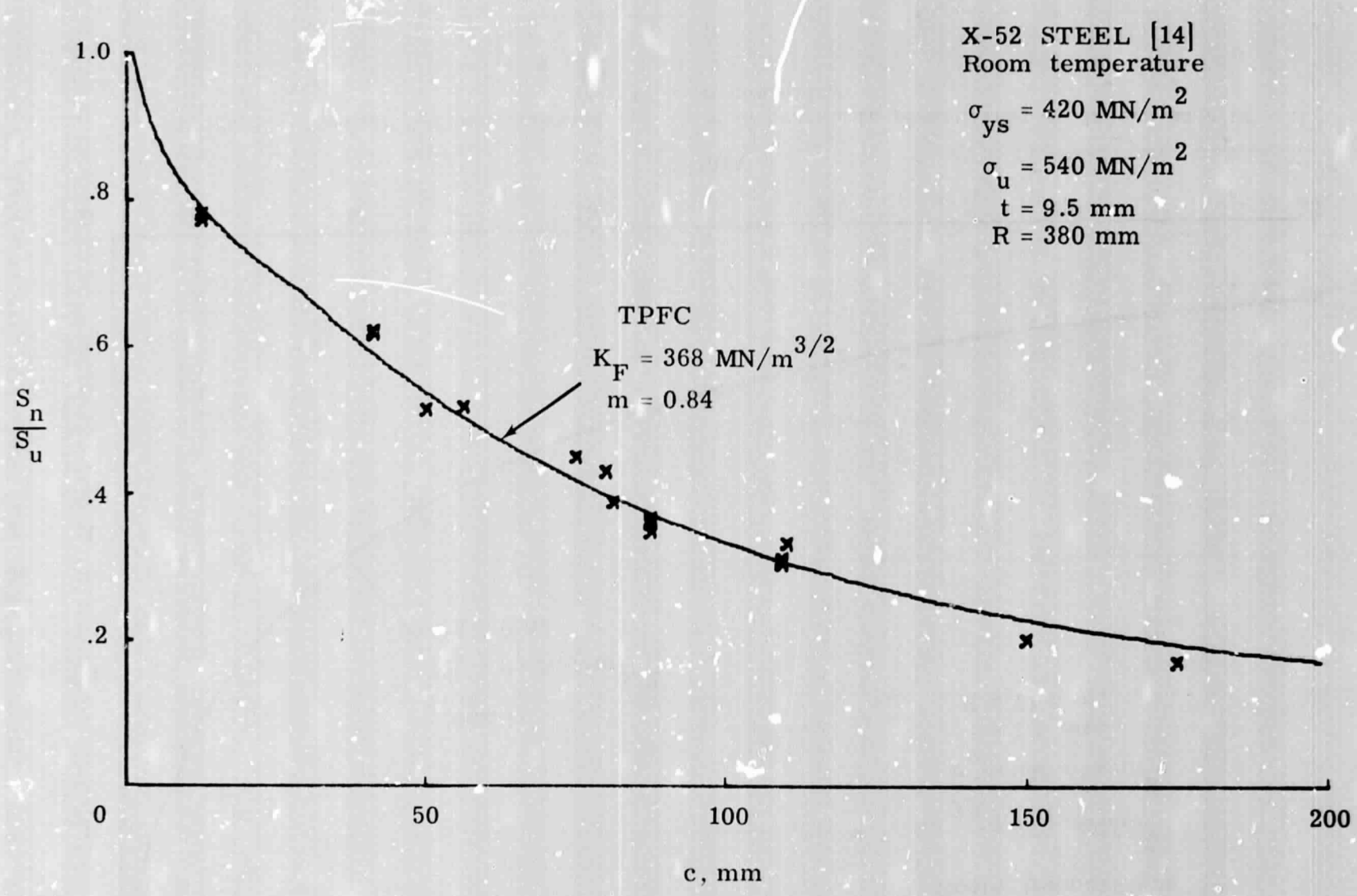

Figure 6.- Nominal failure stresses for through cracks in pressurized cylinders made of X-52 steel.

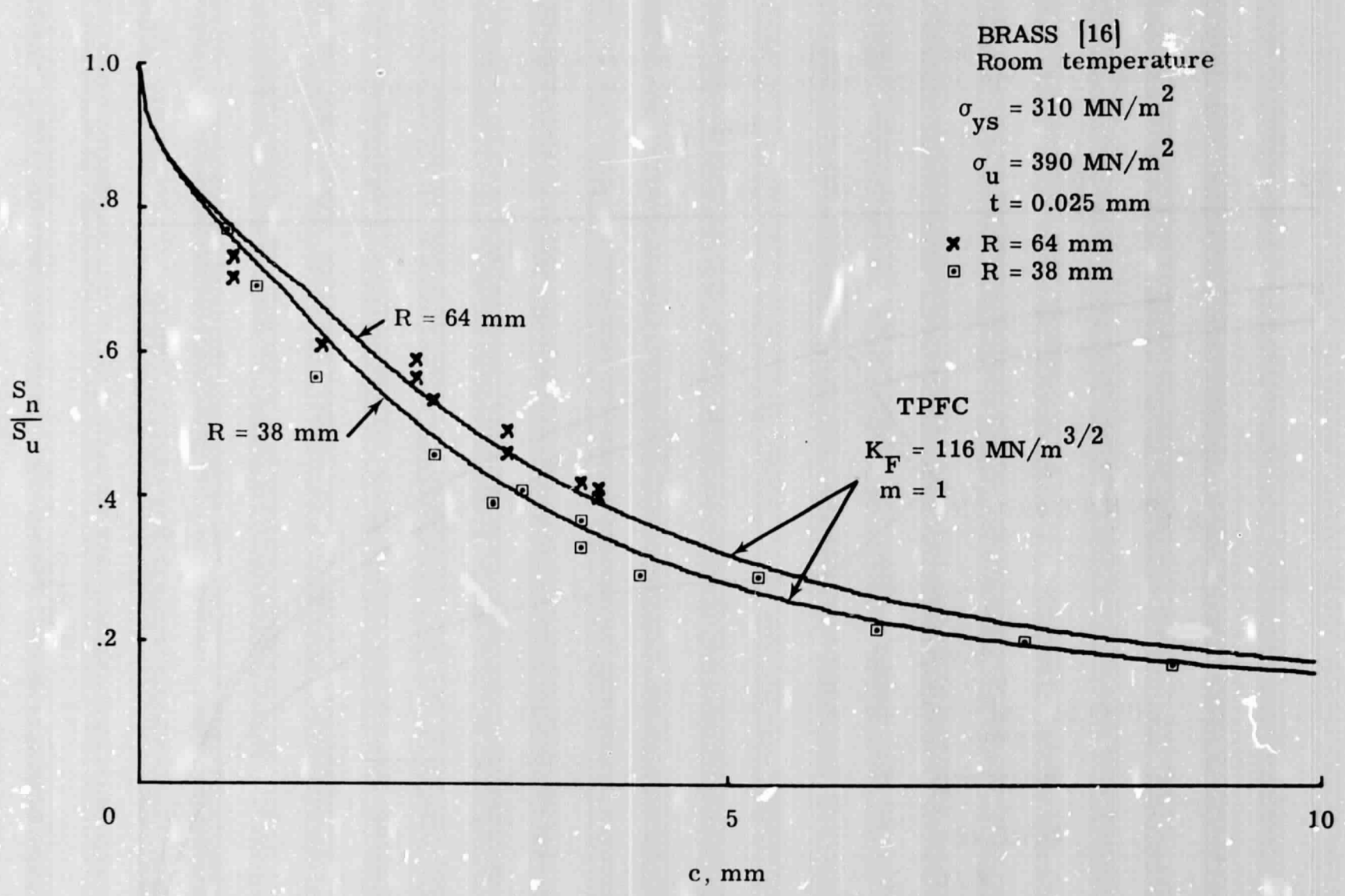

Figure 7.- Nominal failure stresses for through cracks in pressurized cylinders made of brass.

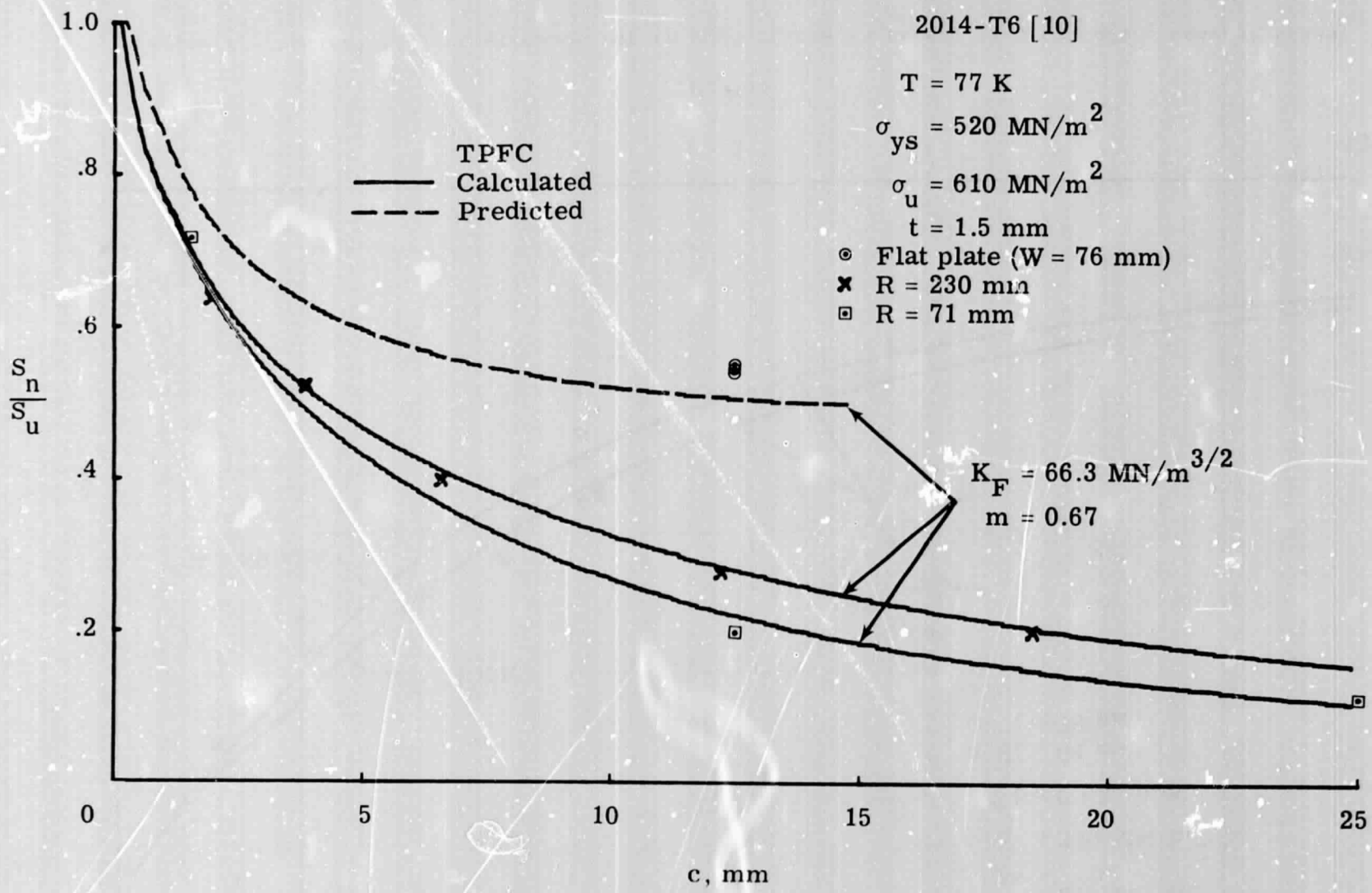

Figure 8.- Nominal failure stresses for through cracks in flat plates and pressurized cylinders made of 2014-T6 aluminum alloy.

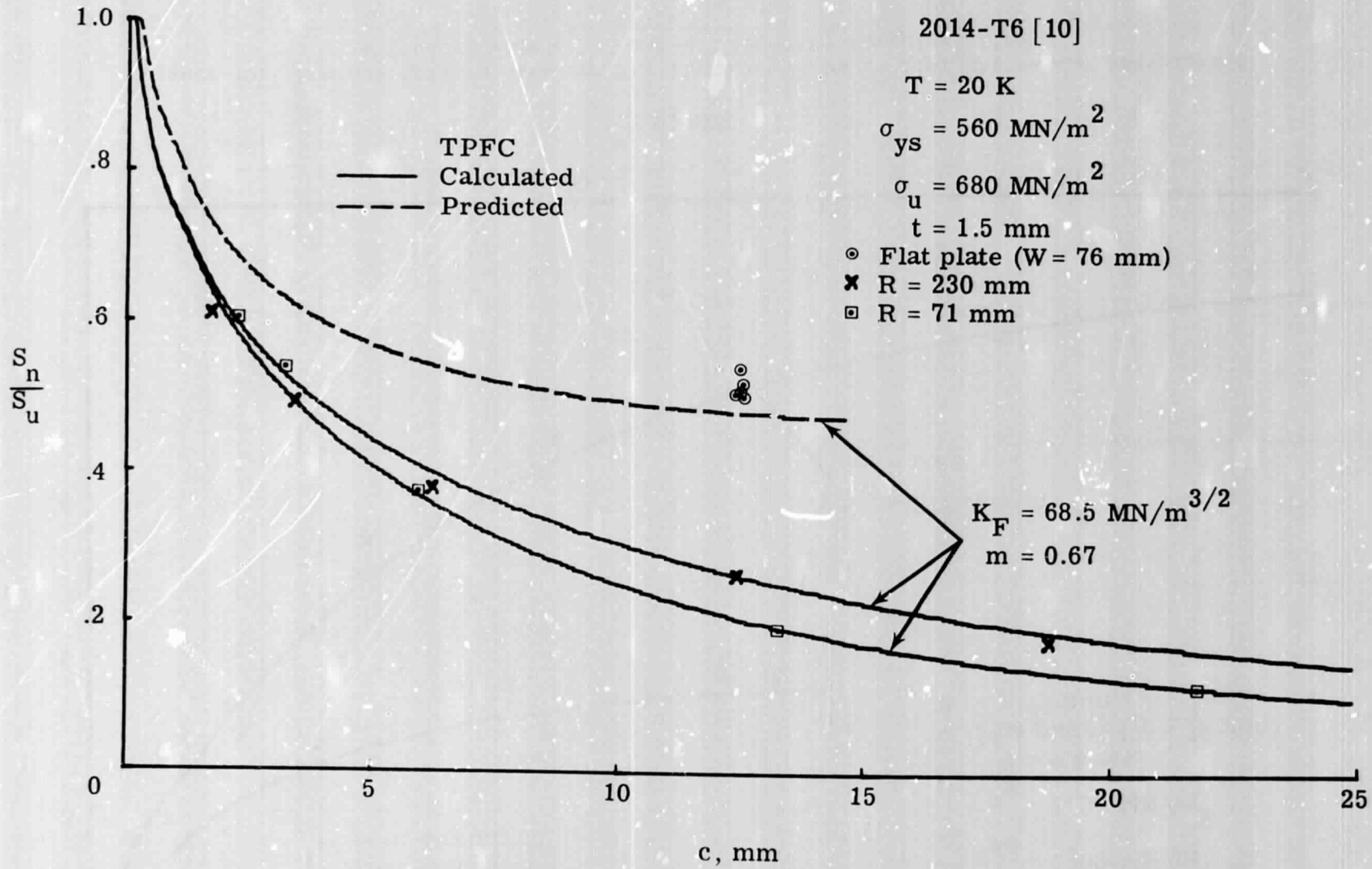

Figure 9.- Nominal failure stresses for through cracks in flat plates and pressurized cylinders made of 2014-T6 aluminum alloy.

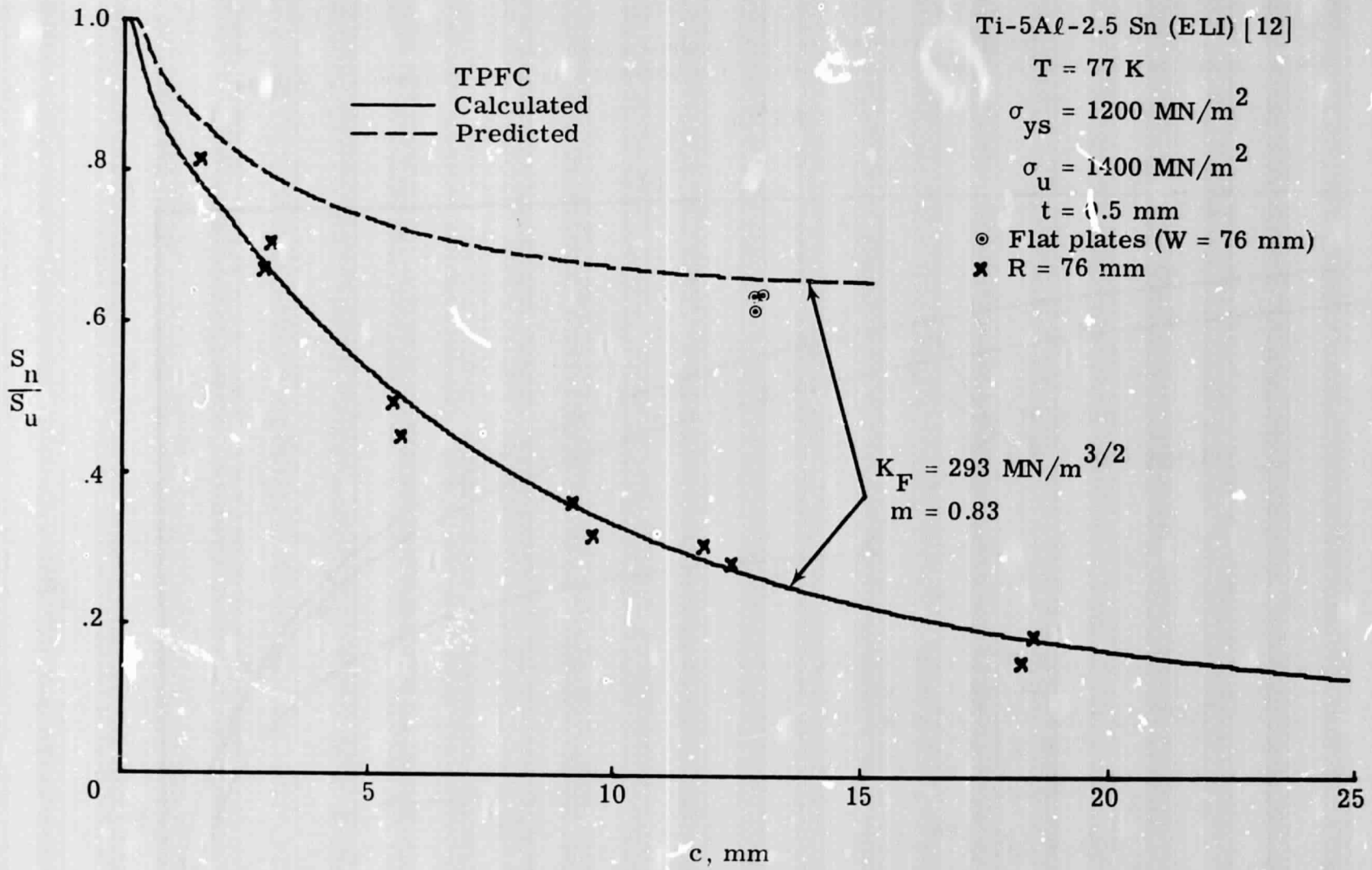

Figure 10.- Nominal failure stresses for through cracks in flat plates and pressurized cylinders made of Ti-5Aℓ-2.5 Sn (ELI) titanium alloy.

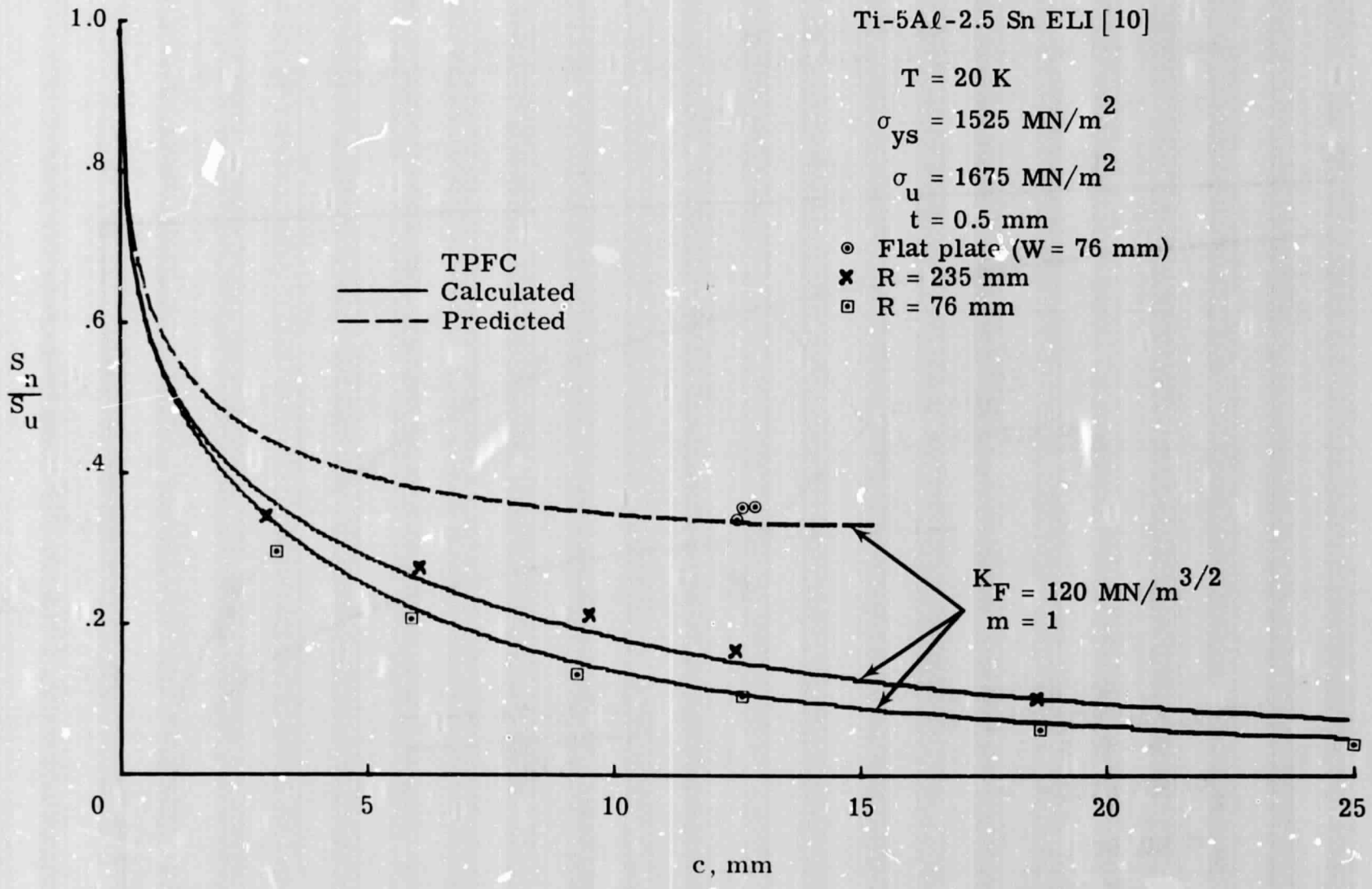

Figure 11.- Nominal failure stresses for through cracks in flat plates and pressurized cylinders made of Ti-5Aℓ-2.5 Sn (ELI) titanium alloy.

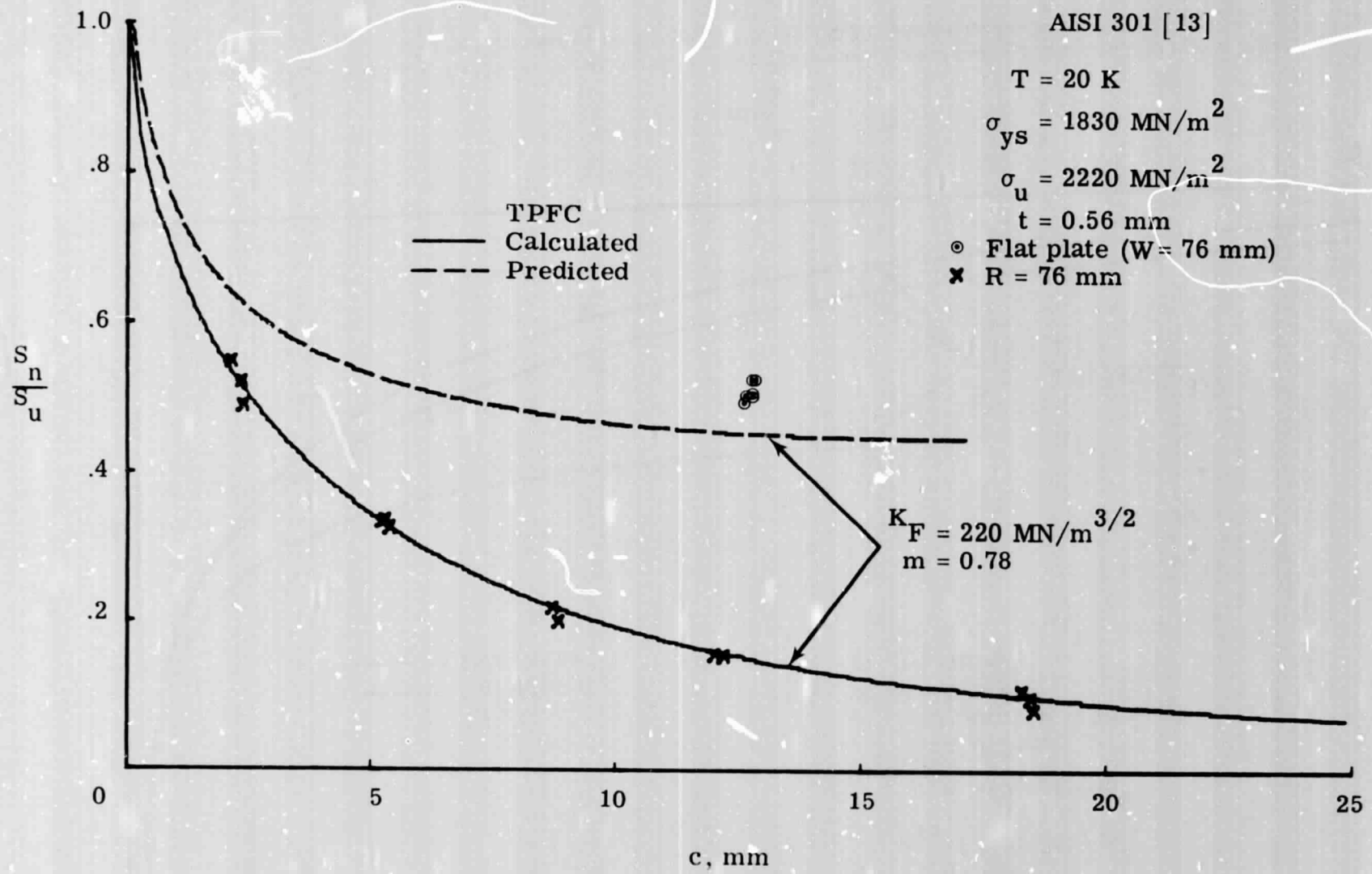

Figure 12.- Nominal failure stresses for through cracks in flat plates and pressurized cylinders made of AISI 301 stainless steel.

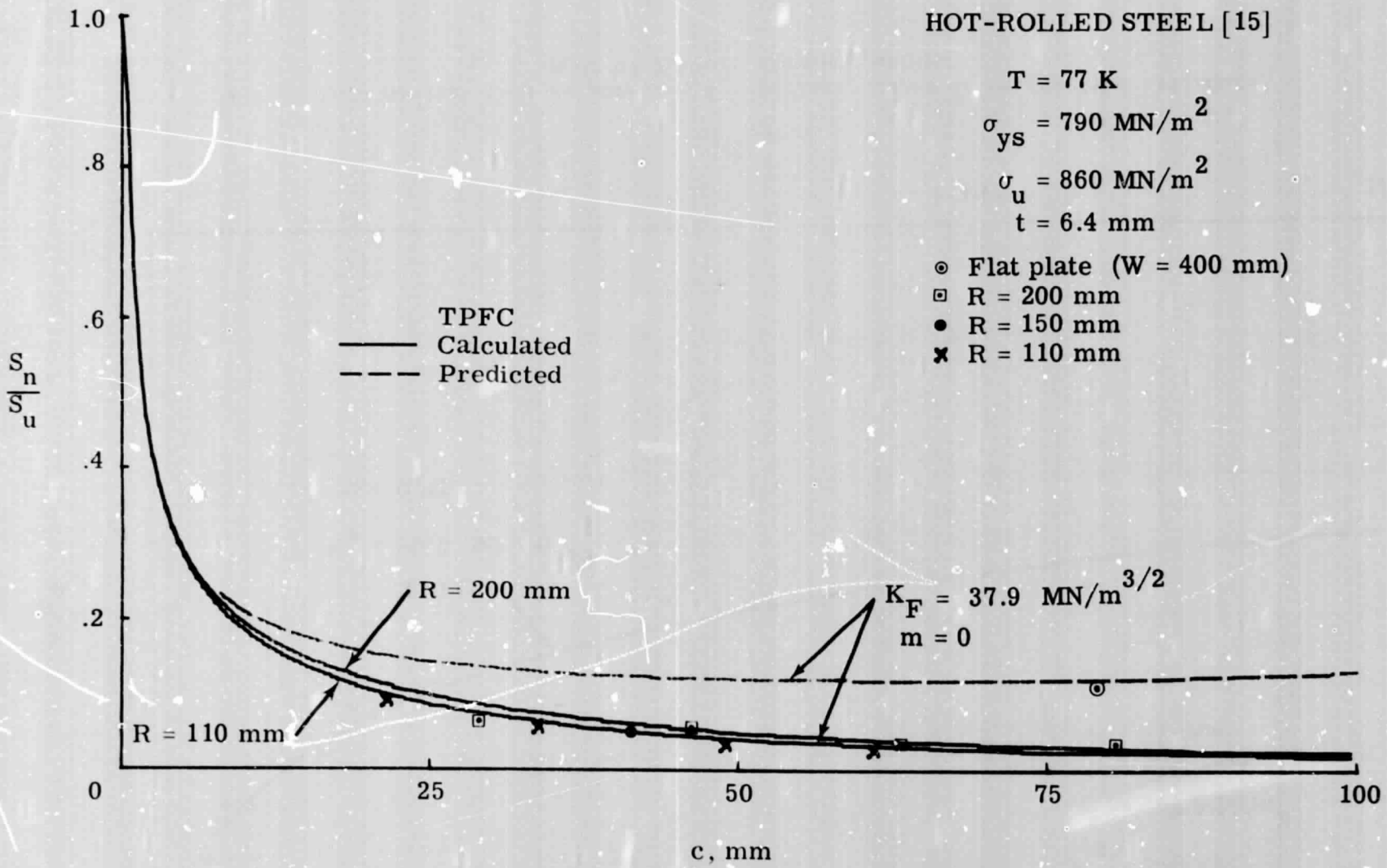

Figure 13.- Nominal failure stresses for through cracks in flat plates and pressurized cylinders made of hot-rolled steel.

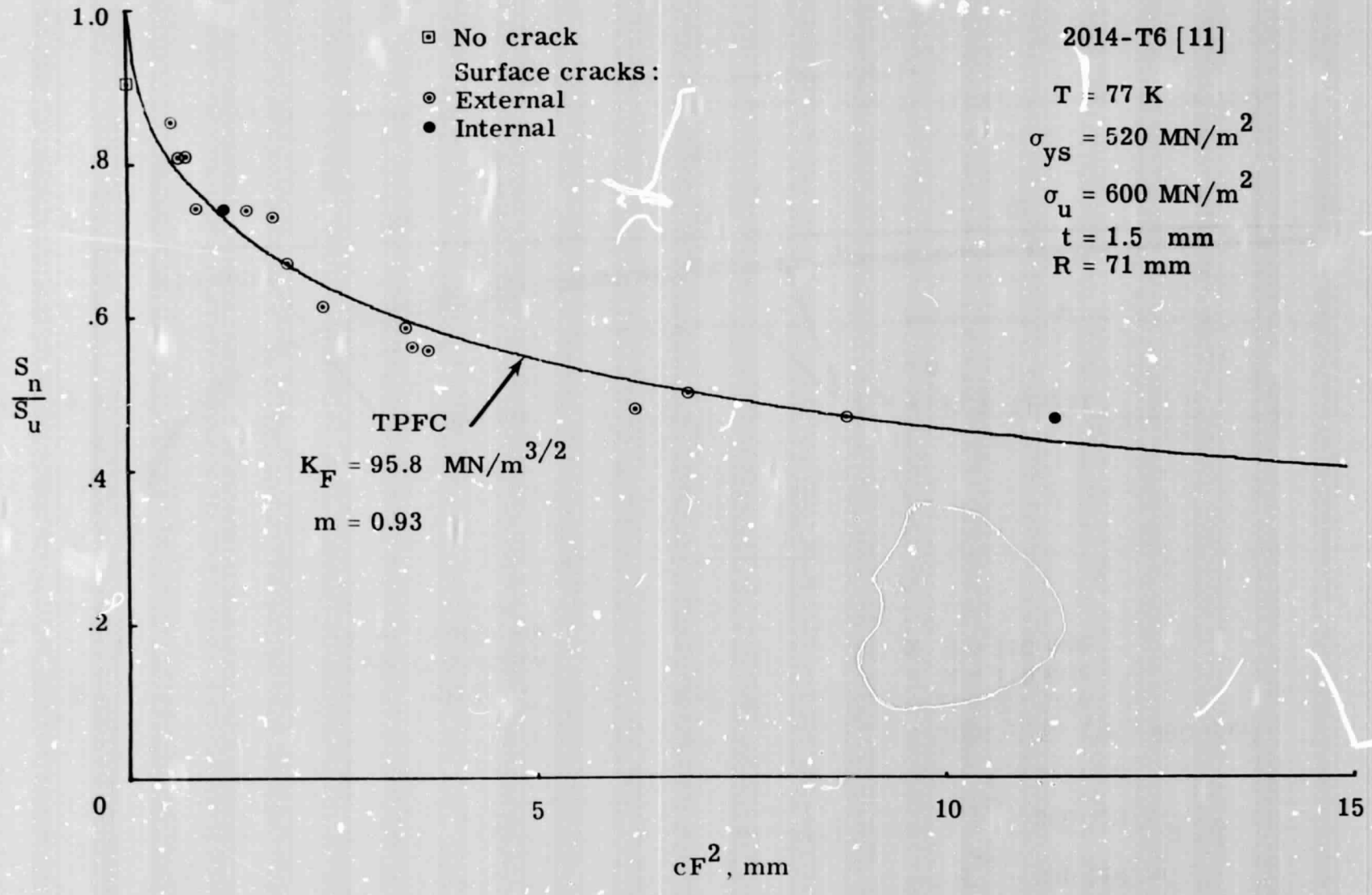

Figure 14.- Nominal failure stresses for surface cracks in pressurized cylinders made of 2014-T6 aluminum alloy.

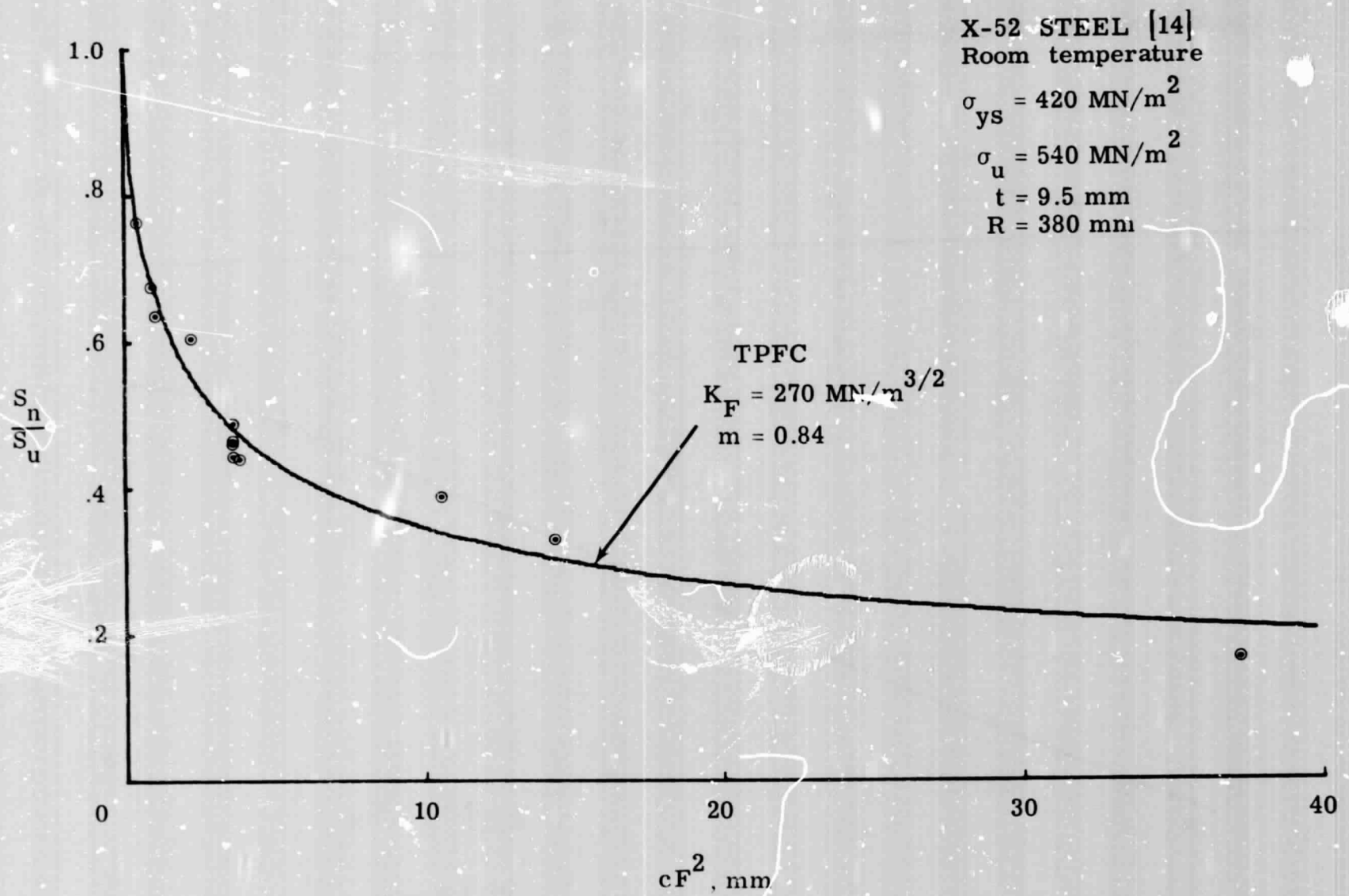

Figure 15.- Nominal failure stresses for surface cracks in pressurized cylinders made of X-52 steel.

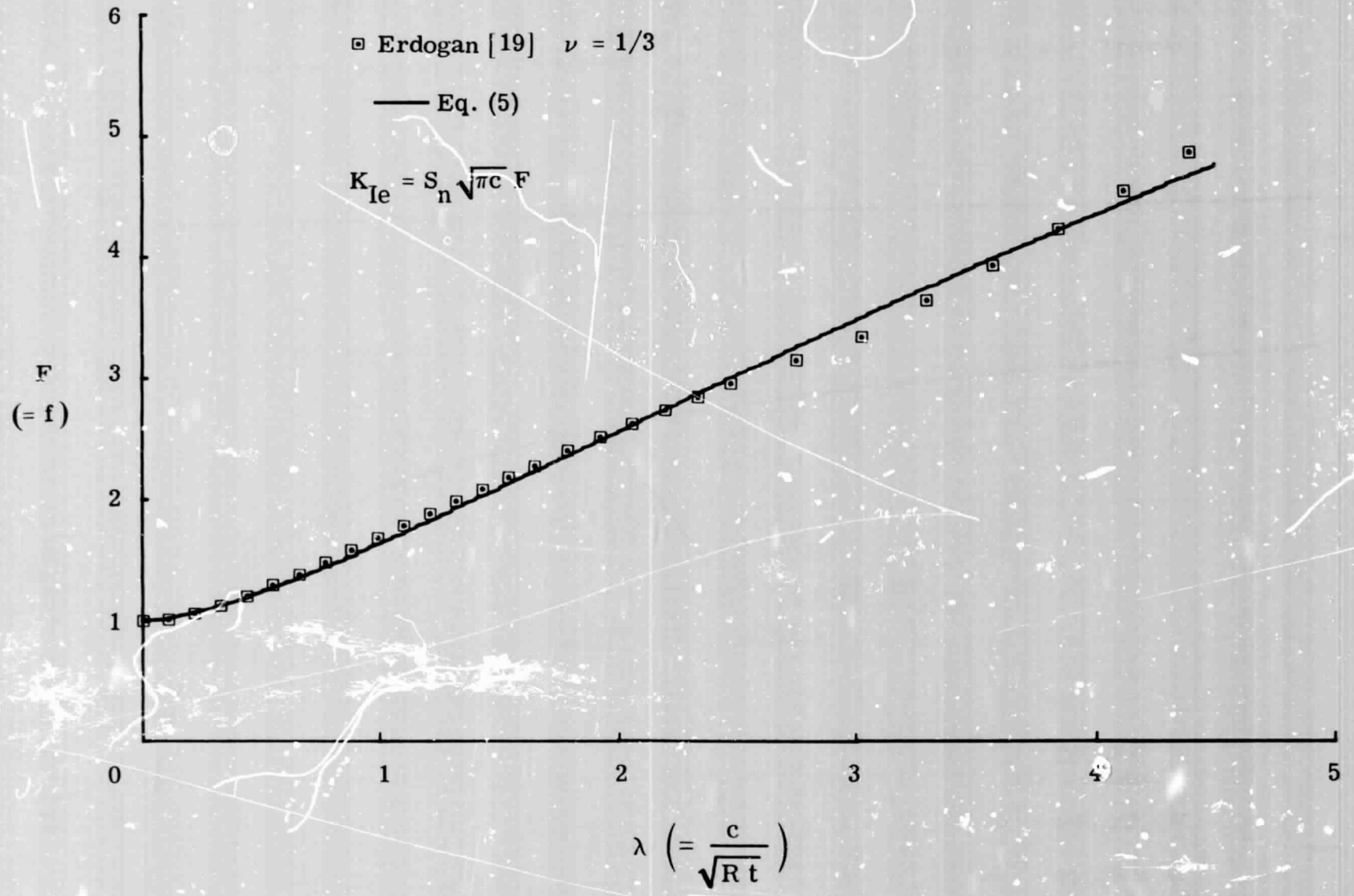

Figure 16.- Shell curvature correction for an axial through crack in a pressurized cylinder.

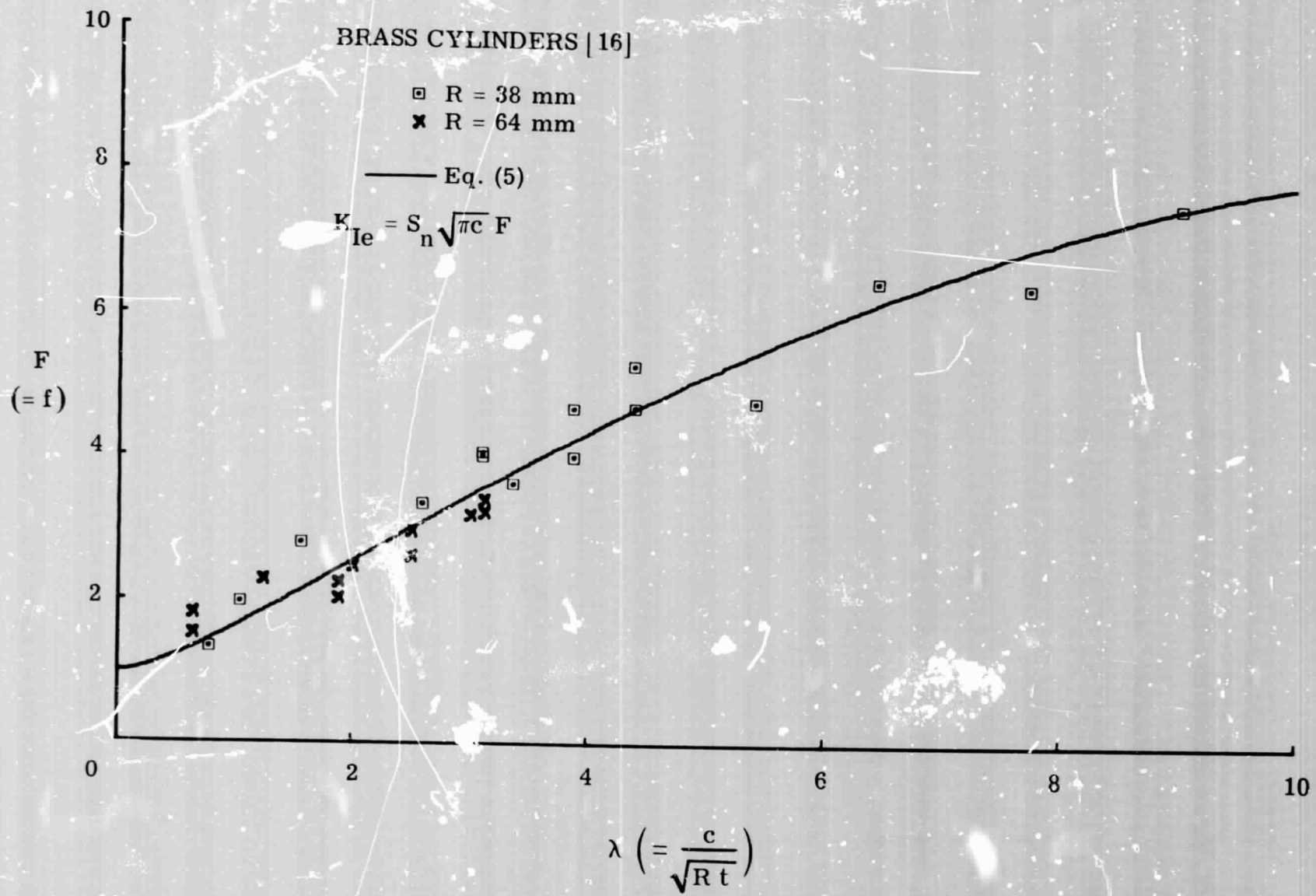

Figure 17.- Experimental and theoretical shell curvature correction for an axial through crack in a pressurized cylinder.